Journal of Neuroendocrinology
From Molecular to Translational Neurobiology

Journal of Neuroendocrinology **24**, 378–392

ORIGINAL ARTICLE

Endothelin-Mediated Calcium Responses in Supraoptic Nucleus Astrocytes Influence Magnocellular Neurosecretory Firing Activity

J. A. Filosa*, K. Naskar*, G. Perfume†, J. A. Iddings*, V. C. Biancardi*, M. S. Vatta† and J. E. Stern*

**Department of Physiology, Georgia Health Sciences University, Augusta, GA, USA.*

†Instituto de Química y Metabolismo del Fármaco-Consejo Nacional de Investigaciones Científicas y Tecnológicas (IQUIMEFA-CONICET), Facultad de Farmacia y Bioquímica, Universidad de Buenos Aires, Argentina.

Journal of Neuroendocrinology

In addition to their peripheral vasoactive effects, accumulating evidence supports an important role for endothelins (ETs) in the regulation of the hypothalamic magnocellular neurosecretory system, which produces and releases the neurohormones vasopressin (VP) and oxytocin (OT). Still, the precise cellular substrates, loci and mechanisms underlying the actions of ETs on the magnocellular system are poorly understood. In the present study, we combined patch-clamp electrophysiology, confocal Ca^{2+} imaging and immunohistochemistry to study the actions of ETs on supraoptic nucleus (SON) magnocellular neurosecretory neurones and astrocytes. Our studies show that ET-1 evoked rises in $[Ca^{2+}]_i$ levels in SON astrocytes (but not neurones), an effect largely mediated by the activation of ET_B receptors and mobilisation of thapsigargin-sensitive Ca^{2+} stores. The presence of ET_B receptors in SON astrocytes was also verified immunohistochemically. ET_B receptor activation either increased (75%) or decreased (25%) SON firing activity, both in VP and putative OT neurones, and these effects were prevented when slices were preincubated in glutamate receptor blockers or nitric oxide synthase blockers, respectively. Moreover, ET_B-mediated effects in SON neurones were also prevented by a gliotoxin compound, and when changes in $[Ca^{2+}]_i$ were prevented with bath-applied BAPTA-AM or thapsigargin. Conversely, intracellular Ca^{2+} chelation in the recorded SON neurones failed to block ET_B-mediated effects. In summary, our results indicate that ET_B receptor activation in SON astrocytes induces the mobilisation of $[Ca^{2+}]_i$, likely resulting in the activation of glutamate and nitric oxide signalling pathways, evoking in turn excitatory and inhibitory SON neuronal responses, respectively. Taken together, our study supports an important role for astrocytes in mediating the actions of ETs on the magnocellular neurosecretory system.

Key words: endothelins, glia, hypothalamus, oxytocin, vasopressin.

doi: 10.1111/j.1365-2826.2011.02243.x

Correspondence to:
Javier E. Stern, Department of Physiology, Georgia Health Sciences University, 1120 15th St Augusta, GA 30912, USA (e-mail: jstern@georgiahealth.edu).

Endothelins (ETs) are a peptide family composed of three isoforms (ET-1, ET-2 and ET-3) and their biological actions are mediated by two well characterised G-protein-coupled receptors: ET_A, which exhibits higher affinity for ET-1 than for ET-2 and ET-3, and ET_B, which displays similar affinity for all three isoforms (1–3). ETs are involved in a wide variety of physiological functions, including regulation of the cardiovascular system. In addition to their potent peripheral vasoactive effects, ETs act as neurotransmitters/neuromodulators within central nervous system regions involved in cardiovascular and fluid balance homeostasis (4–7). Accumulating evidence supports an important role for ETs in the regulation of the hypothalamic magnocellular neurosecretory system, which produces and releases the neurohormones vasopressin (VP) and oxytocin (OT). Both *in vivo* and *in vitro* studies demonstrate that ETs efficiently influence VP and OT secretion from magnocellular neurosecretory cells (MNCs) in the supraoptic (SON) and paraventricular (PVN) hypothalamic nuclei (8–12). However, the actions of ETs on the magnocellular system are highly complex, with both excitatory and inhibitory responses reported. Although most components of the ET system, including the ETs, their receptors and converting enzymes, are present in brain regions involved in the regulation of the magnocellular system (13–15), the specific cellular substrates, loci and mechanisms underlying actions of ETs on MNCs are still poorly understood. For example, i.c.v. microinjections of ETs, or

directly within the subfornical organ (SFO), resulted in the activation of PVN neurones and increased VP release (16,17). These effects were prevented by lesions of the region anteroventral to the third ventricle (11), suggesting that ETs can indirectly stimulate VP release from the SON/PVN by activating excitatory inputs from the SFO. Conversely, direct effects of ETs within the magnocellular system have also been demonstrated, in which ETs can either stimulate or inhibit VP release, depending on the receptor subtype involved (6,18). Thus, although activation of hypothalamic ET_B receptors stimulated both intranuclear somatodendritic, as well as neurohypophyseal VP release, activation of ET_A receptors stimulated or inhibited VP release when acting within the posterior pituitary or the hypothalamus, respectively (9). In addition, electrophysiological studies in hypothalamic slices showed that ETs modulate the firing activity of SON neurones (19,20). Although these studies thus support the direct actions of ETs within the SON/PVN nuclei, the precise cellular targets and mechanisms mediating such effects still remain to be elucidated.

Neurohormone release from the neurohypophysis is highly dependent on the electrical activity of MNCs (21). In addition to intrinsic membrane properties and synaptic mechanisms (22), dynamic neuronal–glial interactions have been shown to play critical roles in the regulation of magnocellular neurosecretory function, both under basal and stimulated conditions, such as dehydration and lactation (23,24). Astrocytic modulation of magnocellular neurosecretory activity involves multiple mechanisms, including dynamic retraction/expansion of processes, regulation of ambient neurotransmitter levels, as well as the release of neuroactive substances, including D-serine, nitric oxide and ATP (25–29). Importantly, ETs and its receptors are present in brain astrocytes (30–35), and numerous functional effects of ETs on astrocytes have been described (30,36–38). Still, whether astrocytes are important components involved in the signalling of ETs within the magnocellular neurosecretory system has not been thoroughly investigated. In the present study, we combined patch-clamp electrophysiology, confocal Ca^{2+} imaging and immunohistochemistry techniques, aiming to study the actions of ETs on both magnocellular neurosecretory neurones and their associated astrocytes. By contrast to a recent study (19), we found that ET-1, mostly through ET_B receptor activation, induces the mobilisation of $[Ca^{2+}]_I$ in SON astrocytes. The results obtained in the present study suggest that this action results in the activation of glutamate and nitric oxide signalling pathways, evoking in turn excitatory and inhibitory SON neuronal responses, respectively.

Materials and methods

Male Wistar rats (weighing 80–140 g) were purchased from Harlan Laboratories (Indianapolis, IN, USA), and housed under a 12 : 12 h light/dark cycle with access to food and water *ad lib.* In a subset of experiments, we also used male heterozygous transgenic vasopressin (AVP)-enhanced green fluorescent protein (eGFP) Wistar rats (n = 7; 5–6 weeks old), in which VP neurones are endogenously fluorescent (39). Founders of this colony were kindly donated by Dr Y. Ueta (University of Occupational and Environmental Health, Kitakyushu, Japan). All procedures were carried out in agreement with Georgia Health Sciences University Committee's guidelines, and in compliance with NIH guidelines.

Brain slice preparation

Hypothalamic slices containing the SON were obtained as described previously (40). Rats were anaesthetised with pentobarbital (50 mg/kg) and perfused through the heart with a cold sucrose solution (containing in mM: 200 sucrose, 2.5 KCl, 3 $MgSO_4$, 26 $NaHCO_3$, 1.25 NaH_2PO_4, 20 D-glucose, 0.4 ascorbic acid, 1 $CaCl_2$ and 2 pyruvic acid (290–310 mOsmol/l). Rats were decapitated, brains were dissected out, and coronal slices (300 and 250 μm for electrophysiology and Ca^{2+} imaging, respectively) obtained in an oxygenated ice-cold artificial cerebrospinal fluid (aCSF) (containing in mM: 119 NaCl, 2.5 KCl, 1 $MgSO_4$, 26 $NaHCO_3$, 1.25 NaH_2PO_4, 20 D-glucose, 0.4 ascorbic acid, 2 $CaCl_2$ and 2 pyruvic acid; pH 7.4; 290–310 mOsmol/l), using a vibroslicer (DSK Microslicer, Ted Pella, Redding, CA, USA). Slices were kept until used in a holding chamber containing aCSF (room temperature). In some cases, as indicated, an aCSF with nominal 0 Ca^{2+}, 3 mM Mg^{2+} and 3 mM ethylene glycol tetraacetic acid (EGTA) was used (41).

Electrophysiological recordings

Once in the recoding chamber, slices were bathed with solutions (approximately 3.0 ml/min) that were continuously bubbled with 95% O_2–5% CO_2 and maintained either at room temperature (approximately 22–24 °C) or at 33–35 °C, as indicated. Conventional whole-cell patch clamp recordings were obtained as described previously (40). Patch pipettes (4–7 MΩ) composed of thin-walled (outer diameter 1.5 mm, inner diameter 1.17 mm) borosilicate glass (GC150T-7.5; Clark, Reading, UK) were pulled on a horizontal electrode puller (P-97; Sutter Instruments, Novato, CA, USA). The internal solution contained (mM): 135 potassium gluconate, 0.2 EGTA, 10 HEPES, 10 KCl, 0.9 $MgCl_2$, 4 MgATP, 0.3 NaGTP and 20 phosphocreatine (Na^+); pH 7.2–7.3. Recordings were obtained with a Multiclamp 700 A amplifier (Axon Instruments, Foster City, CA, USA) using infrared differential interference contrast (DIC) videomicroscopy. The voltage-output was digitised at 16-bit resolution, 10 kHz (Digidata 1320A; Axon Instruments) and saved on a computer for offline analysis. For current-clamp recordings, all protocols were run using an output gain of 10 and a Bessel filter of 10 kHz. Spontaneous firing activity was recorded in continuous mode before, during and after bath application of drugs. Plots of mean firing frequency (bin = 15 s) over time were generated and, for comparison purposes, the mean firing frequency during a period of approximately 3 min before and after drug application was calculated and compared using Mini Analysis software (Synaptosoft Inc., Leonia, NJ, USA). In the case of phasically active neurones, the activity quotient (i.e. the proportion of time in which a cell is active) was used to determine changes in firing activity. Neurones showing a > 30% in firing rate were arbitrarily considered responsive to the drug treatment. Cell input resistance before and during drug applications was calculated in the voltage-clamp mode using a 5-mV pulse when holding the cells at −70 mV. To calculate the delay of drug action, the time at which the drug reached the tissue and the onset of the response were calculated. In the case of astrocyte recordings, Lucifer yellow (0.1 mg/1 μl) was added to the patch pipette solution and, once in the whole-cell configuration, the membrane response to a voltage ramp (from −120 mV to +100 mV, in 600 ms) was assessed.

Immunohistochemistry

Immunohistochemical detection of ET_B receptors in SON neurones and astrocytes was performed using conventional triple immunofluorescence, as described previously (42). Rats (n = 4) were deeply anaesthetised with sodium pentobarbital (100 mg/kg i.p.) and perfused transcardially with 0.01 M phosphate-buffered saline (PBS) (150 ml) followed by 4% paraformaldehyde (350 ml). Brains were post-fixed in 4% paraformaldehyde for 3 h at 4 °C. Fixed brains were cryoprotected at 4 °C with 0.01 M PBS containing

30% sucrose for a minimum of 48 h. Sections (25 μm) were then cut with a cryostat, and incubated in a solution of 0.01 M PBS with 0.1% Triton X-100, NaN_3 0.04% and 10% normal horse serum for 1 h. Sections were incubated overnight in a mix of primary antibodies that included: guinea pig anti-oxytocin; guinea pig anti-VP (dilution 1 : 50 000, each; Bachem, San Carlos, CA, USA), mouse anti-S100b (dilution 1 : 1000; Sigma-Aldrich, St Louis, MO, USA) and a rabbit anti-endothelin receptor type B (dilution 1 : 500; Alomone Labs, Jerusalem, Israel) antibodies. Incubation in primary antibodies was followed by 4 h of incubation in secondary antibodies (donkey anti-guinea pig Cy5 labelled, donkey anti-mouse Cy3 labelled, together with donkey anti-rabbit fluorescein isothiocyanate (FITC)-labelled, dilution 1 : 50, 1 : 250 and 1 : 250 dilutions, respectively). All antibodies were diluted with PBS containing 0.1% Triton X-100 and NaN_3 0.04%. All secondary antibodies were obtained from Jackson ImmunoResearch Laboratories (West Grove, PA, USA). Control experiments were performed by omitting primary or secondary antibodies. Histological sections were examined with a Zeiss LSM 510 confocal microscope system (Carl Zeiss, Oberkochen, Germany). The argon-krypton laser was used to excite the FITC (488 nm) and the Cy3 (545) fluorophores, and the helium-neon laser to excite the Cy5 (633 nm) fluorophores. Fluorescent signal cross-talk among channels was avoided by setting image-acquisition parameters with individually labelled sections, ensuring a lack of 'bleed through' to other channels. To determine co-localisation of various fluorescent markers, a stack of confocal images (five consecutive sections, 1 μm Z-step interval) was obtained from the different fluorophores, and merged. A positive co-localisation was considered by the appearance of yellow (red + green) or purple (red + blue) profiles in the merged image. Figures were composed using Adobe Photoshop CS (Adobe Systems, Inc., San Jose, CA, USA).

To obtain a comparison of neuronal and astroglial cells surface areas within the SON, hypothalamic slices were incubated in a cocktail containing a guinea pig anti-oxytocin followed by respective secondary antibodies (see above). Confocal images were taken, and the surface area of immunoidentified oxytocin and vasopressin neurones, and S100β astroglial cells, were measured by manually tracing each cell using Image Pro plus software (Media Cybernetics, Bethesda, MD, USA).

Preabsorption controls were run to test the specificity of the anti-endothelin receptor type B primary antibody (CEMLR KKSGM QIALN D; Alomone Labs), using procedures described previously (43). The antigen and antibody were used at either a concentration of 1.6 μg/ml each, or with an antigen concentration five-fold greater than that of the primary antibody. The mixtures were incubated in in PBS containing 0.1% Triton X-100 and NaN_3 0.04% for 2 h at room temperature, centrifuged for 5 min at 10 000 *g*, and the supernatants applied to the tissue, in accordance with the procedure described above.

Confocal calcium imaging

Measurements of changes in intracellular Ca^{2+} levels in SON astrocytes were performed using live confocal imaging techniques, as described previously (44). Because of lower imaging resolution from adult rat brains, imaging experiments were conducted in rats postnatal day 25 (P25) $\pm$ 5. Ca^{2+} imaging was performed using the Andor Technology Revolution system (Andor Technology, South Windsor, CT, USA) [iXON EMCCD camera with the Yokogawa CSU 10, confocal scanning unit (Yokogawa, Tokyo, Japan)]. This unit is attached to a Zeiss microscope (Axioscope 2FS). Slices were incubated at room temperature in aCSF containing 10 μM Fluo4-AM or Rhod2-AM and pluronic acid (2.5 μg/ml). After 1 h of incubation, slices were washed and placed in aCSF at room temperature until needed. Slices were loaded in batches so that they could be used within the same time frame after the loading procedure. At the time of the experiment, a slice was transferred to a perfusion chamber on the microscope and held with a nylon grid and continuously superfused with aCSF at 33–35 °C. Fluorescence images were obtained using a krypton/argon laser at 488 nm and emitted light at > 495 (Fluo4) or 561 nm and emitted > 607 nm (Rhod2). Dye-loading into SON neurones was achieved by the addition of Fluo-5F pentapotassium salt (100 μM) into the internal pipette solution. Once the whole-cell configuration was established, the dye was allowed to dialyse into the cell for at least 10 min before acquisition. Images were acquired at 1–4 frame/s for 8–10 min, depending on the experimental protocol. Ca^{2+} imaging data was analysed using Andor IQ 2.1 software. Fractional fluorescence (F/F_0) was determined by dividing the fluorescence intensity (F) within a region of interest by a baseline fluorescence value (F_0) determined from approximately 50 images showing no activity. To compare responsive astrocytes among treatments, the percentage of identified astrocytes (i.e. cells loaded with Fluo4/Rhod2 before stimulus application) that displayed an increase in intracellular Ca^{2+} during the treatment was calculated. Cells with large somas and punctate staining, as well as a defined nucleus/nucleolus, were excluded from the analysis because they represented dead neuronal cell bodies, confirmed in DIC illumination.

Chemicals

All chemicals were obtained from Sigma-Aldrich, with the exceptions of ET-1 (American Peptide, Sunnyvale, CA, USA), BQ-788 (Tocris, Ellisville, MO, USA), L-NAME (Alexis Biochemicals, San Diego, CA, USA), Fluo4-AM and Rhod2-AM (Invitrogen, Carlsbad, CA, USA) and Sarafotoxin (EMD, San Diego, CA, USA).

Statistical analysis

All values are expressed as the mean $\pm$ SEM. Nonparametric unpaired (Mann–Whitney), paired (Wilcoxon) tests, or one-way ANOVA were used, as needed. $P < 0.05$ was considered statistically significant. All statistical analyses were conducted using GRAPHPAD PRISM (GraphPad Software, San Diego, CA, USA).

Results

ET-1 increases $[Ca^{2+}]_I$ levels in SON astrocytes via the release of Ca^{2+} from intracellular stores

In addition of being capable of synthesising and releasing ETs, astrocytes also express ET_A and ET_B receptors, making them key candidates for ET signalling in the SON. To determine whether ETs can signal astrocytes, we monitored changes in astrocytic Ca^{2+} activity in SON slices exposed to 10 or 100 nM ET-1. Astrocytes were identified using a combination of approaches. Slices incubated either in Fluo4 or Rhod2 preferentially loaded small cells and processes (putative astrocytes), resulting in a characteristic homogenous staining pattern. Although Fluo4 in some cases also labelled large neuronal profiles, staining in the latter was characteristically punctate and, when observed under DIC illumination, corresponded in most cases to dead neurones located at the surface of the slice. When Rhod2 loading was performed in slices obtained from AVP-eGFP rats (in which VP neurones are endogenously fluorescent), a clear segregation between the loaded putative astrocytes and VP neurones was observed (Fig. 1A). Moreover, we found a large degree of colocalisation between Rhod2 and Fluo4 when both dyes were loaded simultaneously (Fig. 1B). The mean surface area of Rhod2/Fluo4 stained cells was 56.3 $\pm$

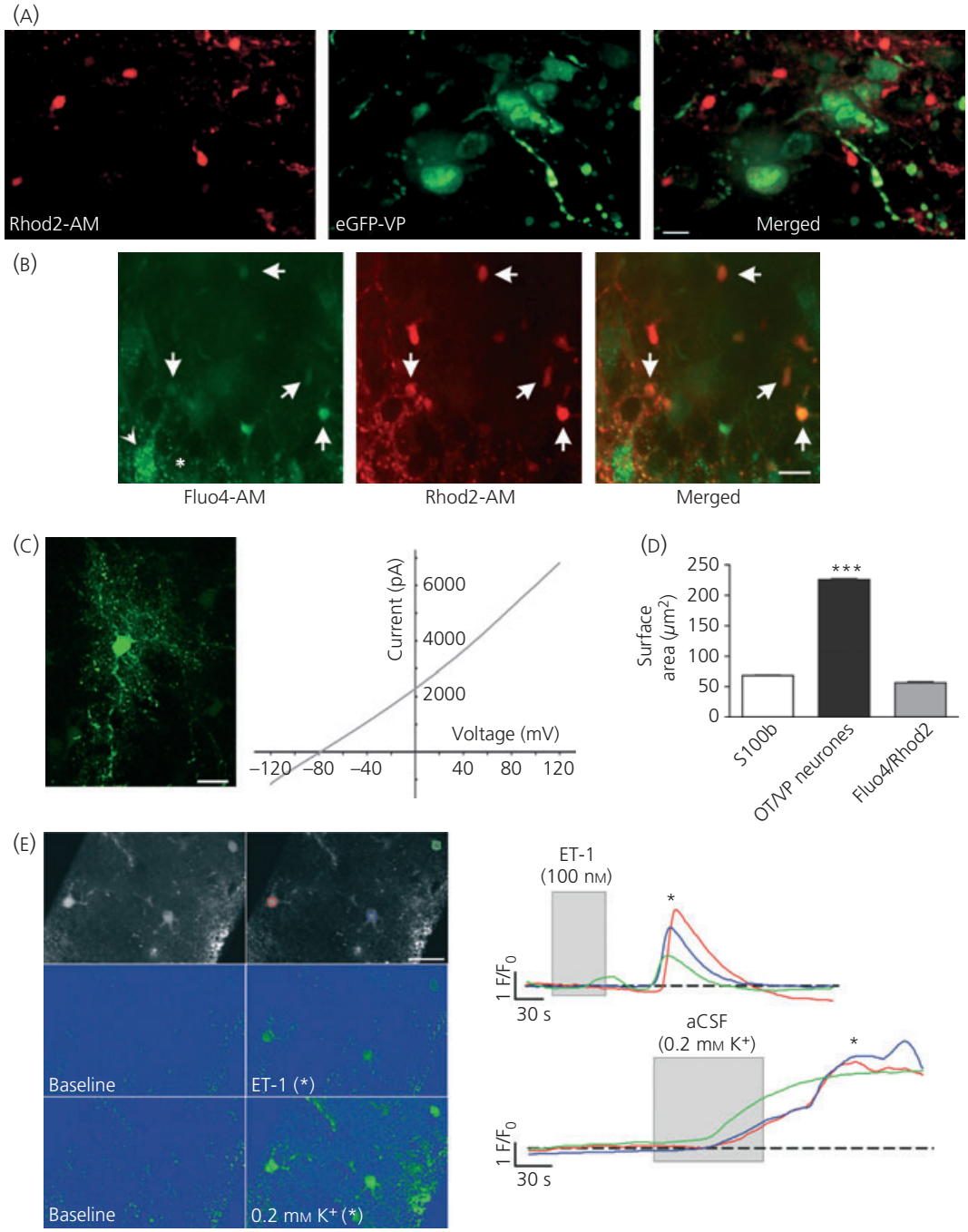

Fig. 1. Characterisation and identification of supraoptic nucleus (SON) astrocytes. (A) SON brain slice from an vasopressin (AVP)-enhanced green fluorescent protein (eGFP) rat loaded with the Ca^{2+} indicator dye Rhod2-AM (red, left), vasopressin eGFP fluorescence (green, middle) and merged channels (right). Scale bar = 13 μm. (B) Image of an SON slice loaded with the Ca^{2+} indicator dyes Rhod2-AM (red) and Fluo4-AM (green). Arrows point to examples of Rhod-2/Fluo-4 double-labelled astrocytes. The arrowhead points to a punctate Fluo4-AM staining in a neurone. Note the absence of staining in the majority of large empty spaces, corresponding to unlabelled neurones (see asterisk as an example). Scale bar = 16 μm. (C) Representative Lucifer yellow loaded SON astrocyte and its corresponding current/voltage relationship graph. Scale bar = 10 μm. (D) Summary data of the surface area of cells showing homogeneous loading for Fluo4/Rhod2, compared to those immunostained against S100b or oxytonin (OT)/vasopressin (VP). (E) Upper left, greyscale image of a Fluo-4 loaded SON slice showing labelled astrocytes; the upper right image is a replicate image showing the regions of interest on the astrocytes corresponding to the Ca^{2+} trace shown on the right. Middle and bottom panels are pseudocolour images showing changes in Ca^{2+} fluorescence (F/F_0) before and during stimulation with endothelin (ET)-1 or a low K^+ (0.2 mM) artificial cerebrospinal fluid solution (aCSF). ***P < 0.001 versus S100b and Fluo4/Rhod2. Scale bar = 15 μm.

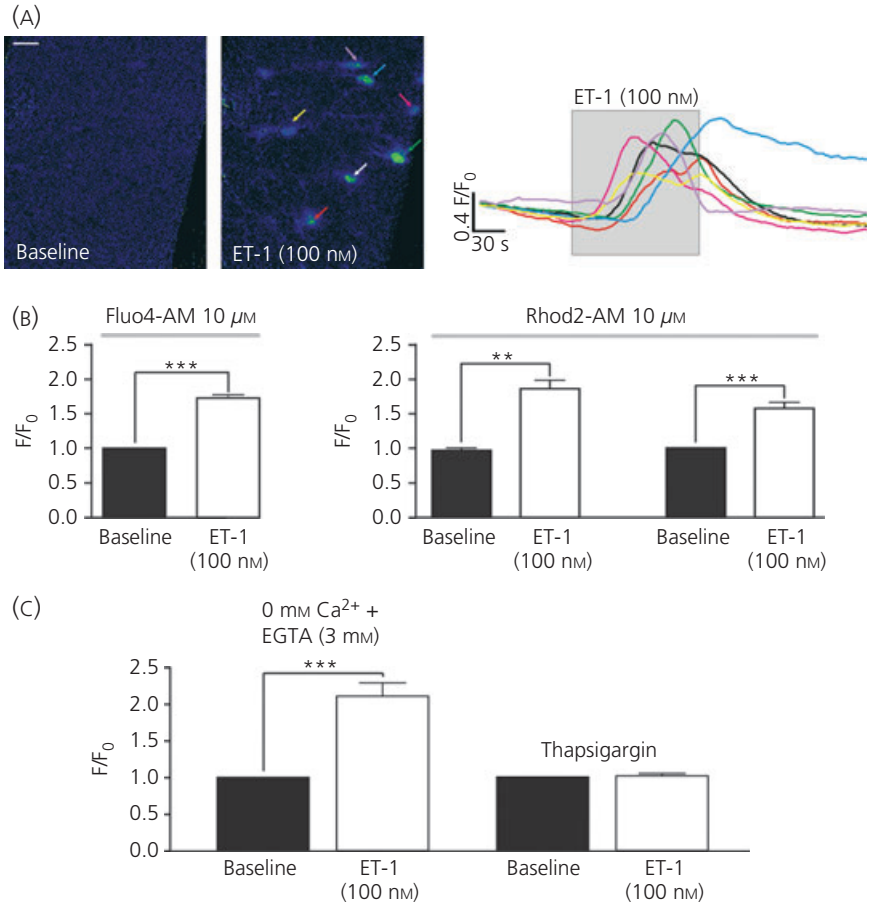

Fig. 2. Endothelin (ET)-1-induced Ca^{2+} responses in astrocytes and dependence on intracellular Ca^{2+} stores. (A) Representative pseudocolour images and corresponding traces from an supraoptic nucleus (SON) slice showing changes in Ca^{2+} fluorescence (F/F_0) before, during and after ET-1 stimulation. (B) Summary data showing mean changes in $\Delta F/F_0$ after ET-1 (10 and 100 nM) exposure in slices loaded either with Fluo4-AM or Rhod2-AM. **P < 0.02 and ***P < 0.001. Scale bar = 10 μm. (C) ET-1-induced Ca^{2+} transients were present in the absence of extracellular Ca^{2+} but were blocked by thapsigargin (3 μM). ***P < 0.0001. Scale bar = 10 μm. EGTA, ethylene glycol tetraacetic acid.

1.75 μm^2 (n = 132), which was similar to that obtained in immunoidentified astrocytes (S100b staining; 68.3 ± 0.8 μm^2, n = 408), with both values being significantly smaller than that obtained in immunoidentified oxytocin and VP neurones (225.9 ± 1.7 μm^2, n = 1453, P < 0.0001, one-way ANOVA) (Fig. 1D). In addition, we found that exposing slices to a low K^+ (0.2 mM) aCSF increased Ca^{2+} in Fluo4 loaded cells (Fig. 1E), previously shown to be a characteristic response of astrocytes but not neurones (45). Finally, to more conclusively demonstrate the identity of the monitored cells as astrocytes, we patched and recorded currents from putative astrocyte profiles, at the same time as loading them with Lucifer yellow (n = 6). As shown in the representative example (Fig. 1C), we found in all cases a linear current/voltage relationship over an extended range of voltages, a membrane behaviour characteristic of astrocytes, but not neurones. Moreover, the intracellular staining revealed complex and ramified fine processes, which typically surrounded large cell bodies within the SON (Fig. 1C, asterisk). Based on all of these approaches, we can conclude that Fluo4/Rhod2 loaded cells are astrocytes.

As shown in Figs 1(E) and 2(A,B), ET-1 (100 nM) elicited significant transient increases in SON astrocytic $[Ca^{2+}]_i$ levels both in Fluo4 (F/F_0 from 1.01 ± 0.001 to 1.72 ± 0.05, n = 131, P < 0.0001, Wilcoxon test) and in Rhod2 labelled astrocytes (F/F_0 from 0.97 ± 0.03 to 1.86 ± 0.12, n = 6, P < 0.03, Wilcoxon test). Similar results were observed when 10 nM ET-1 was tested (F/F_0 from 1.00 ± 0.001 to 1.57 ± 0.09, n = 11, P < 0.001, Wilcoxon test), an effect that was not significantly different from that observed with ET-1 100 nM. On average, ET-1-induced peak Ca^{2+} responses occurred with a delay of 79.68 ± 8.01 s from the time the drug reached the microscope chamber.

To determine the source of Ca^{2+} mediating ET-1 responses, experiments were repeated in the absence of extracellular Ca^{2+}, or after depletion of intracellular Ca^{2+} stores with thapsigargin. In the absence of extracellular Ca^{2+}, ET-1 elicited significant increases in astrocytic $[Ca^{2+}]_I$ (F/F_0 from 1.00 ± 0.006 to 2.11 ± 0.18, n = 34, P < 0.0001, Wilcoxon test). Conversely, no changes were observed in slices pre-incubated (45 min) with thapsigargin (3 μM, F/F_0 from 1.003 ± 0.002 to 1.02 ± 0.034, n = 8, P > 0.2) (Fig. 2C). Taken

together, these results support intracellular Ca^{2+} stores as being the main Ca^{2+} source for ET-1-induced responses in SON astrocytes.

Contribution of ET_B receptors to ET-1-mediated increases in $[Ca^{2+}]_I$ in SON astrocytes

We then aimed to determine the type of receptors mediating ET-1 effects on astrocytic Ca^{2+}. We found that, similar to ET-1, the ET_B selective receptor agonist sarafotoxin 6c (S6c, 100 nM) evoked an increase in astrocytic $[Ca^{2+}]_i$ levels in Fluo4 (F/F_0 from 1.01 ± 0.001 to 1.47 ± 0.04, n = 22, P < 0.0001, Wilcoxon test) and Rhod2 loaded slices (F/F_0 from 1.01 ± 0.002 to 2.12 ± 0.2, n = 22, P < 0.0001, Wilcoxon test) (Fig. 3A). On average, S6c-induced peak Ca^{2+} responses occurred with a delay of 62.8 ± 5.4 s from the time the drug reached the microscope chamber. The mean proportion of responsive astrocytes was significantly higher in the S6c group (100%) compared to ET-1 (approximately 75%, P > 0.05, Bonferroni's post-hoc test, one-way ANOVA) (Fig. 3C). Further

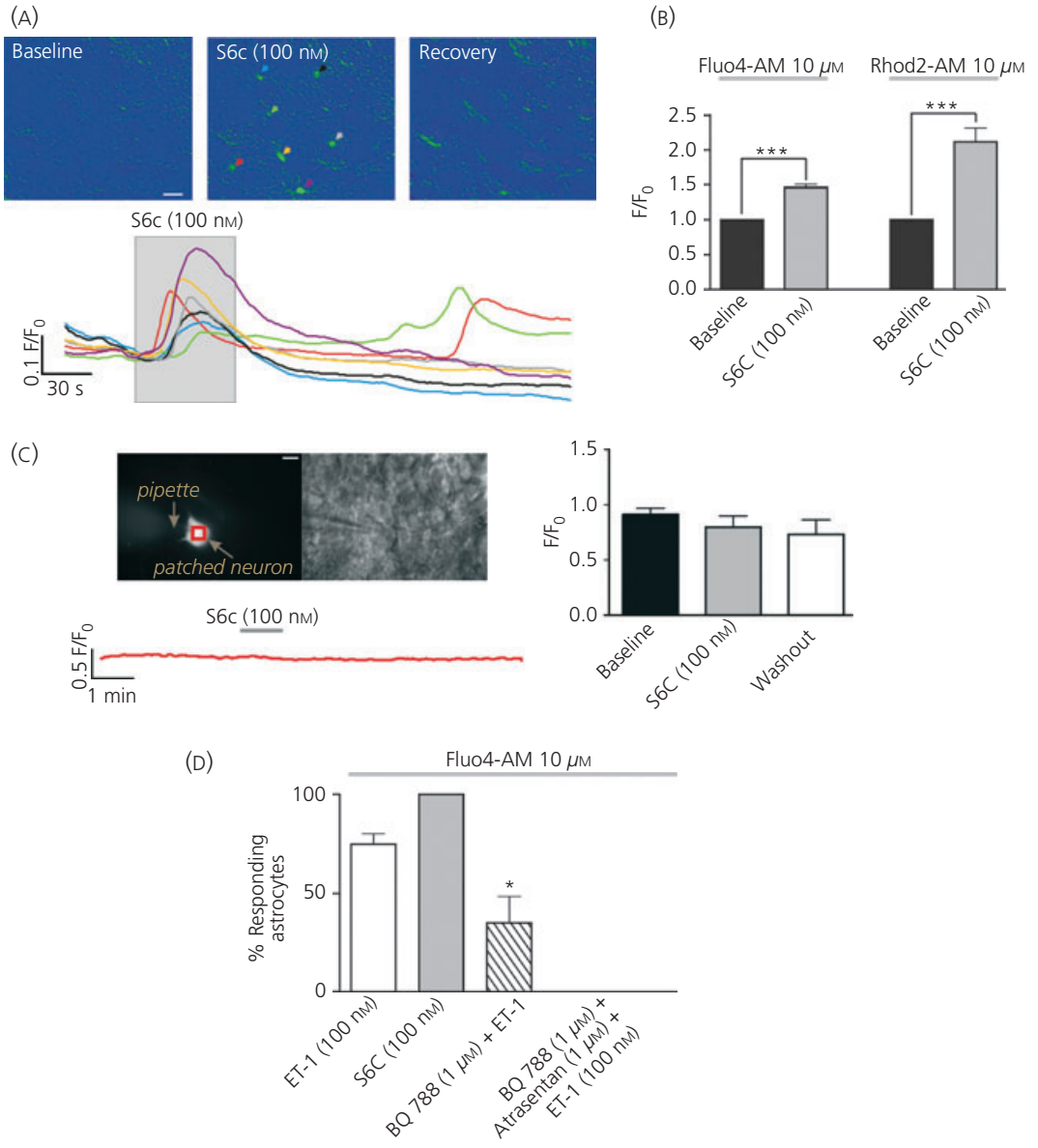

Fig. 3. Endothelin (ET)-1-induced Ca^{2+} changes in astrocytes are largely mediated by activation of ET_B receptors. (A) Representative pseudocolour images of transient Ca^{2+} changes in astrocytes induced by the ET_B receptor agonist S6c. The corresponding traces are shown below. (B) Summary data of $\Delta F/F_0$ in response to S6c in slices loaded with Fluo4-AM or Rhod2-AM. (C) Patched supraoptic nucleus (SON) neurone loaded with Fluo5F (left) and corresponding differential interference contrast image (right). No changes in $\Delta F/F_0$ were observed when stimulated with S6c, as shown in the trace below and the summary data. Scale bar = 15 μm. (D) Percentage of responding astrocytes to ET-1, Sarafotoxin 6c (S6c) and ET-1 in the presence of the ET_B receptor blocker BQ-788 or the ET_B and ET_A receptor blockers BQ-788 and atrasentan. *** P < 0.0001. *P < 0.01 versus ET-1 and Sc6, Bonferroni's post-hoc test, one-way ANOVA. Scale bars = 10 μm.

confirming a contribution of ET_B receptors in SON astrocytes, we found that, in the presence of the selective ET_B receptor blocker BQ-788 (1 μM) (46), the proportion of ET-1-responsive astrocytes was largely diminished ($P < 0.01$ versus ET-1 and Sc6, Bonferroni's post-hoc test, one-way ANOVA) (Fig. 3D). The magnitude of the $[Ca^{2+}]_i$ changes of responsive astrocytes, however, was not affected (F/F_0 from 1.0 ± 0.001 to 1.60 ± 0.07, $n = 13$, $P < 0.0005$, Wilcoxon test). Finally, responses to ET-1 were completely blocked, in the presence of a cocktail containing the ET_B receptor blocker BQ-788 and the selective ET_A receptor blocker atrasentan (1 μM) (Fig. 3D).

To determine whether activation of ET_B receptors also evoked neuronal Ca^{2+} responses, we intracellularly loaded SON neurones with Fluo5F through a patch pipette in the whole-cell patch configuration. Given that ET-1 may affect SON firing activity in a Ca^{2+}-independent manner (see below), and that action potentials *per se* can efficiently increase intracellular Ca^{2+}, these experiments were conducted in the presence of tetrodotoxin (0.5 μM). By contrast to what we observed in astrocytes, bath application of ET-1 failed to evoke Ca^{2+} transients in SON neurones (F/F_0 from 0.93 ± 0.43 to 0.83 ± 0.8, $n = 4$, $P = 0.13$, Wilcoxon test) (Fig. 3C).

Finally, in an attempt to rule out a potential contribution of ET-mediated vasoconstriction on astrocyte Ca^{2+} changes, ET-1-induced stimulation was repeated in the presence of papaverine (100 μM), previously reported to block ET-mediated vasoconstrictions (47). Our results show that, in slices pre-incubated with papaverine for 15 min, astrocyte Ca^{2+} responses to ET-1 (100 nM) were still observed (F/F_0 from 1.00 ± 0.005 to 1.5 ± 0.05, $n = 36$, $P < 0.0001$, Wilcoxon test).

ET_B receptor activation influences the firing activity of MNCs

Given previous studies supporting a major role of ET_B receptor in CNS astrocytes (36,38,48), the subsequent electrophysiological studies were focused on this specific receptor subtype. To determine whether activation of ET_B receptors also affected the neuronal excitability of magnocellular neurosecretory neurones, patch-clamp recordings were obtained from SON neurones ($n = 55$) in the current-clamp mode. Mean series resistance and input resistance were 21.7 ± 2.3 MΩ and 1.1 ± 0.2 GΩ, respectively.

In a first set of experiments, we evaluated whether bath application of S6c (100–300 nM, 3.5 min) affected ongoing firing activity. Recordings were obtained either at room temperature ($n = 15$) or at 32–35 °C ($n = 9$). Because similar results were obtained under both conditions, data were pooled for simplicity, and data were analysed according to the firing pattern displayed by the recorded neurones [i.e. continuous ($n = 20$) or phasic ($n = 4$)]. Excitatory responses to S6c were observed in the majority (14/20, 70%) of continuously firing neurones (84.3 ± 16.3% increase in firing, $P < 0.0001$, Wilcoxon test) (Fig. 4A). Inhibitory responses were observed in most of the other neurones (5/20, 63.4 ± 4.2% inhibition, $P < 0.05$, Wilcoxon test) (Fig. 4B), whereas a lack of response was observed in one continuously firing cell. Similar proportions of excitatory and inhibitory responses to S6c were observed in phasically active neurones. Thus, whereas excitatory responses were observed in 3/4 (75%) neurones (55.4 ± 25.5% increase) (Fig. 4C), an inhibitory response was observed in the remaining neurone. The low number of observations prevented us from performing a statistical comparison in this group of neurones.

In a different set of studies, we used AVP-eGFP rats, in which VP neurones can be readily identified based on their endogenous fluorescence (39). Recordings (at 33–35 °C) were obtained from eGFP-positive ($n = 9$) and eGFP-negative ($n = 7$) neurones. Within the eGFP-positive group, excitatory responses to S6c were observed in the majority of the neurones (6/9, approximately 70%) (44.2 ± 12.7% increase in firing, $P < 0.03$, Wilcoxon test), whereas inhibitory responses where observed in the remaining neurones (3/9, approximately 30%) (-70.6 ± 7.4% decrease in firing). In the eGFP-negative group, we found excitatory responses to 100 nM S6c in 4/7 (approximately 60%) of neurones (77.6 ± 14.3% increased firing, $P < 0.05$, Wilcoxon test), whereas inhibitory responses were observed in the remaining 3/7 neurones (62.1 ± 16.9% decrease in firing) (Fig. 4D). The low number of observations in the inhibited groups prevented us from performing statistical comparisons.

Finally, we found that, in neurones showing an excitatory response to S6c, neuronal input resistance (measured in voltage-clamp at a holding potential of −75 mV) decreased significantly after S6c application (from 1.32 ± 0.26 GΩ to 0.90 ± 0.11 GΩ, $P < 0.02$, Wilcoxon test). A similar decrease was also observed in neurones showing an inhibitory response to S6c (from 1.27 ± 0.29 GΩ to 0.64 ± 0.09 GΩ, $P < 0.01$, Wilcoxon test).

By contrast to astrocytic Ca^{2+} responses, changes in neuronal firing rate after ET_B receptor activation occurred after a relatively long delay (6.2 ± 0.6 min). No differences in response latency were observed between neurones showing excitatory (6.1 ± 0.8 min) or inhibitory (6.4 ± 0.4 min) responses ($P > 0.05$, Mann–Whitney test). In most cases, the effects of S6c on neuronal activity showed no recovery within the recording period, suggesting that ETb receptor activation in the SON evokes relatively long lasting effects on magnocellular neurones.

Are ET_B-induced changes in SON firing activity dependent on an astrocyte-mediated mechanism?

Given the time course differences in the ET_B-evoked responses between SON astrocytes and neurones, we tested whether neuronal responses were dependent on, or mediated by, an astrocyte-dependent mechanism. Accordingly, electrophysiological recordings of SON neurones were repeated in the presence of the gliotoxin-selective compound L-αAA (49–51), a commonly used method to temporarily disable astrocytic function (52–55). We have previously shown that this approach blocks astrocytic Ca^{2+} transients in response to different stimuli, including extracellular electrical stimulation (56) and activation of metabotrophic glutamate receptors (JA. Filosa, unpublished data). Our results show that bath application of S6c in slices preincubated with L-αAA ($n = 8$, 250 μM) failed to evoke any change in SON firing discharge ($P = 0.5$, Wilcoxon test). The results are summarised in Fig. 5(A,B). These results suggest that functional

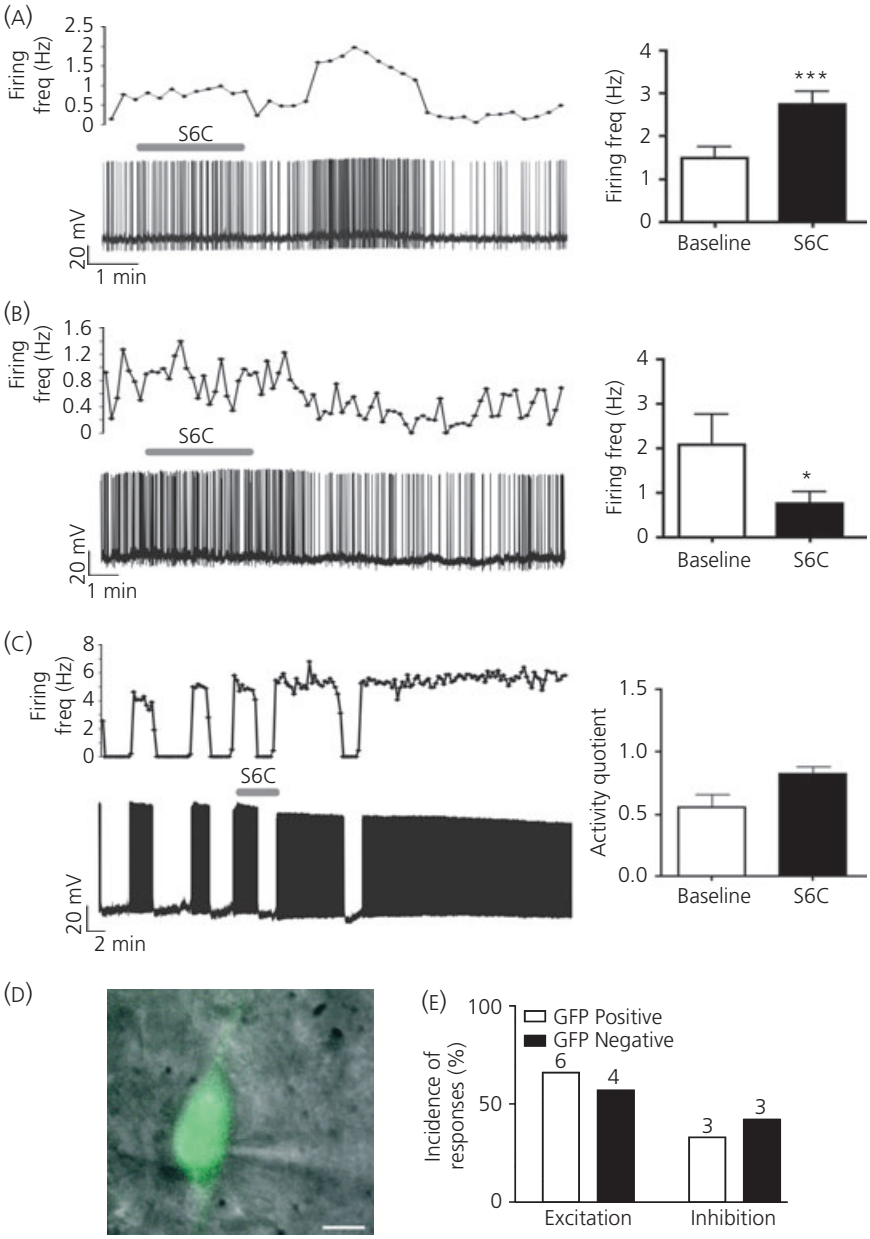

Fig. 4. Endothelin $(ET)_B$ receptor activation altered the firing activity in supraoptic nucleus (SON) neurones. (A) Representative trace, corresponding mean firing frequency plot (bin = 10 s) and summary data showing Sarafotoxin 6c (S6c, 100 nM)-mediated excitatory effects in continuously active SON neurones (n = 14). (B) Representative trace, corresponding mean firing frequency plot (bin = 10 s) and summary data showing Sarafotoxin 6c (S6c, 100 nM)-mediated inhibitory effects in continuously active SON neurones (n = 5). (C) Representative trace, corresponding mean firing frequency plot (bin = 10 s) and summary data showing ET_B receptor-mediated excitatory effects in phasically active SON neurones (n = 3). (D) Representative example of a patched enhanced green fluorescent protein (eGFP)-vasopressin (VP) neurone (left) and summary data showing the incidence of S6c-mediated excitatory and inhibitory responses in eGFP positive and negative SON neurones. The numbers on the bars indicate the number of observations in each group. *P < 0.05 and ***P < 0.0001. Scale bar in (D) = 10 μm.

astrocytes are needed for ETs to evoke a change in SON neuronal activity.

To determine whether neuronal responses to ET_B receptor activation were dependent on changes in $[Ca^{2+}]_i$, experiments were repeated in the presence of BAPTA, a fast Ca^{2+} chelator. In a first set of experiments, recorded SON neurones (n = 8) were intracellularly loaded with BAPTA (10 mM) through the recording patch pipette. Under this condition, S6c continued to evoke a change in firing activity (7/8 = excitation, % change = 308.5 ± 124.5, P < 0.05, Wilcoxon test) similar in magnitude to that evoked under normal conditions (P > 0.05, Mann–Whitney test). These results indicate that the effects of ET_B on SON firing discharge do not result from a direct, Ca^{2+}-dependent effect on the recorded neurone. We then tested whether ET_B responses were affected in slices

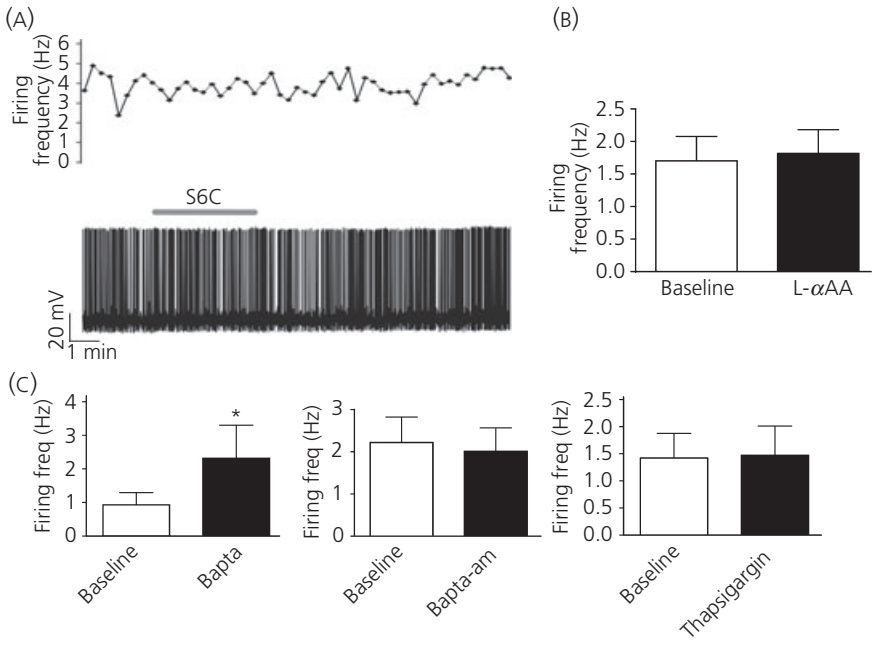

Fig. 5. Inhibition of glial function and chelation of intracellular Ca^{2+} prevented endothelin $(ET)_B$ receptor-mediated changes in supraoptic nucleus (SON) firing activity. (A) Representative trace and corresponding mean firing frequency plot (bin = 10 s) showing a lack of response to S6c (100 nM) in the presence of the gliotoxin L-αAA (250 μM). The mean data (n = 8) are summarised in (B). (C) Summary data showing S6c responses in the presence of BAPTA in the patch pipette (10 mM, n = 8) (left panel), in slices preincubated in BAPTA-AM (20 μM, n = 5) (middle panel) and in slices preincubated in thapsigargin (3 μM, n = 5) (right panel). *P < 0.05.

preincubated with BAPTA-AM (20 μM) to chelate Ca^{2+} both in neurones and astrocytes. Under this condition, and similar to that observed with the gliotoxin, S6c application failed to induce a significant change in SON firing discharge (n = 5, P > 0.05, Wilcoxon test). Similarly, no neuronal responses to S6c application were evoked when slices were preincubated in thapsigargin (3 μM, 45 min, n = 5). The results are summarised Fig. 5(C).

Nitric oxide and glutamate contribute to ET_B receptor-induced inhibition and stimulation of the firing activity of MNCs

Nitric oxide and glutamate are two major neurotransmitters known to inhibit and stimulate, respectively, SON neuronal activity, which are capable of being produced and released by astroglial cells (57–59). Thus, we aimed to determine their potential involvement in ET_B-receptor mediated modulation of SON neuronal excitability. In the presence of the nonselective nitric oxide synthase (NOS) blocker L-NAME (100 μM), no inhibitory responses to S6c application were observed. Most neurones (10/11) displayed excitatory responses (P < 0.001, Wilcoxon test) (Fig. 6), whereas one neurone was nonresponsive. Conversely, in the presence of the selective glutamate AMPA and NMDA receptor blockers DNQX (30 μM) and AP5 (100 μM), only 1/9 neurones showed an excitatory response to S6c, with the rest being either inhibited (7/9; P < 0.01,Wilcoxon test) or nonresponsive (2/9). When combined together, however, no significant differences were observed (n = 9, P > 0.1, Wilcoxon test). Finally, when both NOS and glutamate receptor blockers were combined together, S6c failed to evoke any differences in firing activity (n = 6, P > 0.1, Wilcoxon test).

ET_B receptors are expressed both in SON neurones and astrocytes

Using confocal immunohistochemistry, we found a robust ET_B receptor immunoreactivity in the SON. Staining was found both in the main SON area, as well as in the ventral glial lamina, an area enriched with astroglial cells (Fig. 7A). Preabsorption of the antibody with the corresponding antigen, as well as omission of primary antibody, resulted in a lack of immunostaining (Fig. 7C). To confirm whether ET_B receptors were indeed expressed both in SON neurones and astrocytes, we performed triple immunofluoresence experiments combining antibodies raised against ET_B, S100b (an astroglial marker) and VP. As shown in (Fig. 7A,B), ET_B staining was found both in neurones and astroglial cells. Interestingly, ET_B immunoreactivity in neurones appeared to be predominantly located in the nucleus, as well as perinuclearly.

Discussion

A growing body of evidence supports ETs as being critical players in the central control of cardiovascular and fluid homeostasis. This functionally relevant action of ETs is partly mediated through the modulation of the activity of MNCs and hormone release from the posterior pituitary. Still, the precise mechanisms underlying the actions of ETs on MNCs are poorly understood. In the present

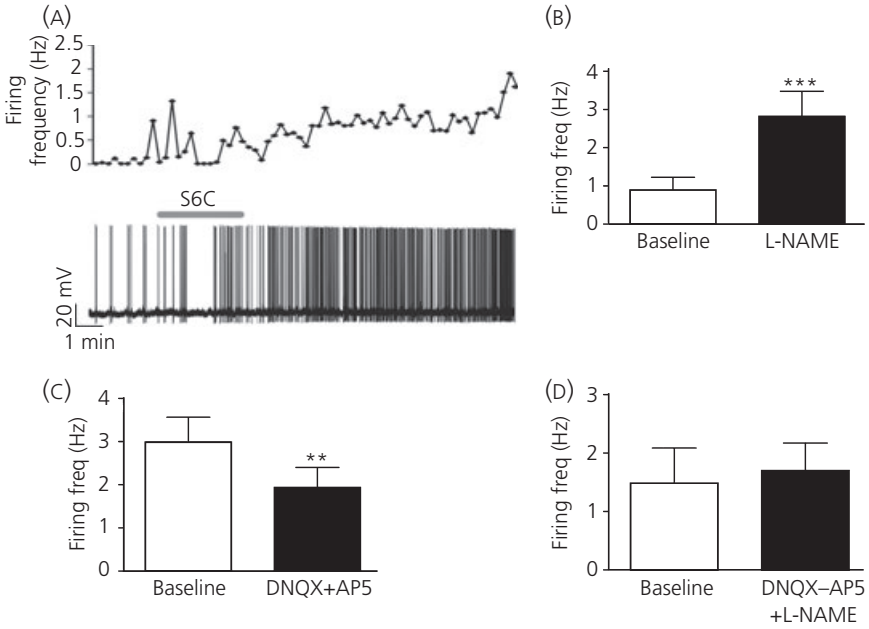

Fig. 6. Nitric oxide synthase (NOS) blockade prevented endothelin $(ET)_B$ receptor-mediated inhibitory responses in supraoptic nucleus (SON) neurones. (A) Representative trace and corresponding mean firing frequency plot (bin = 10 s) showing an excitatory response to S6c (100 nM) in the presence of the NOS blocker L-NAME (100 μM). Summary data for the effects of S6c in the presence of 100 μM L-NAME (n = 10), 30 μM DNQX + 100 μM AP5 (n = 7) and the combination of L-NAME + DNQX + AP5 (n = 6) are shown in (B), (C) and (D), respectively. **P < 0.01 and ***P < 0.001.

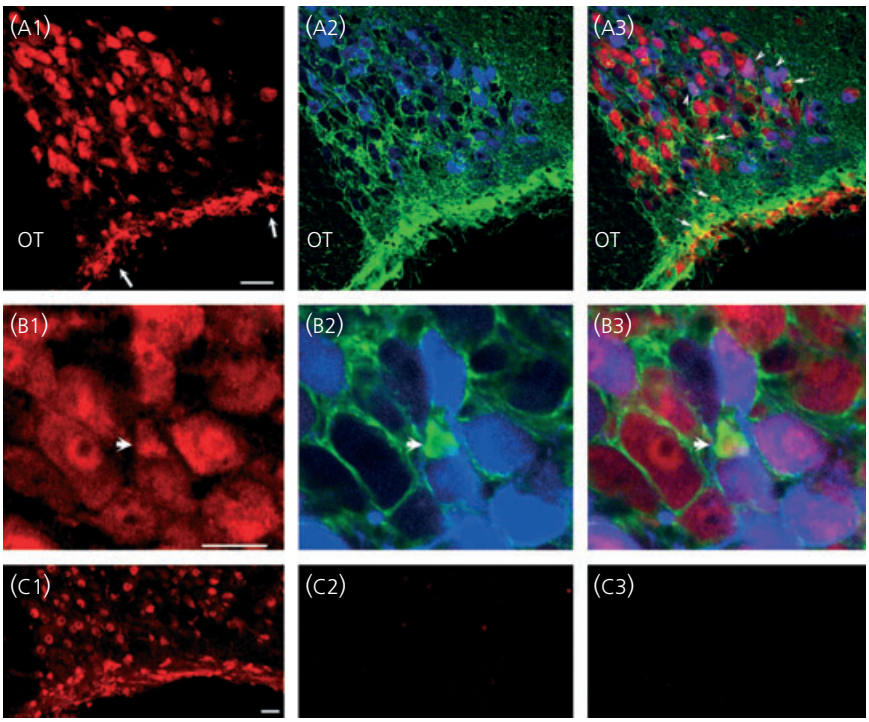

Fig. 7. Endothelin $(ET)_B$ receptor immunoreactivity is present in supraoptic nucleus (SON) neurones and astrocytes. (A) Representative example of ET_B receptor (A1, red), vasopressin and S100b (A2, blue and green, respectively) immunoreactivities in the SON. Note the dense ET_B and S100b immunoreactivities in the ventral glial lamina (region between arrows in A1). In (A3), both images are superimposed to better display colocalisation of ET_B and vasopressin (VP) (arrowheads, purple) and ET_B and S100b (arrows, yellow). (B) A representative example from another section is shown at higher magnification. The arrowhead points to an example of an S100b positive astrocyte, displaying positive ET_B receptor immunoreactivity. (C) Representative examples showing ET_B receptor immunoreactivity in the SON (C1), and absence of staining after either preabsorption of the antibody with the corresponding antigen (C2), or removal of primary antibody from incubation (C3). Scale bars: (A) = 20 μm, (B) = 15 μM, (C) = 50 μm. OT, optic tract.

study, we aimed to shed light into the mechanisms of actions of ETs, using a combination of patch-clamp electrophysiology, Ca^{2+} imaging and immunohistochemistry. The main findings that emerge from our studies can be summarised: (i) ET-1 evoked rises in $[Ca^{2+}]_i$ levels in SON astrocytes (but not neurones), effects that involved the activation of ET_A and ET_B receptors and the mobilisation of thapsigargin-sensitive Ca^{2+} stores; (ii) ET_B receptor activation evoked excitatory (75%) and inhibitory (25%) responses in MNC firing activity, effects likely mediated by glutamate and nitric oxide, respectively; (iii) ET_B-mediated actions in MNCs were abolished when a selective gliotoxin compound was used, and when mobilisation of $[Ca^{2+}]_i$ was prevented with bath-applied BAPTA-AM or thapsigargin. Conversely, intracellular Ca^{2+} chelation in the recorded MNC failed to block ET_B-mediated effects. Taken together, our results suggest that ET_B receptor activation in SON astrocytes induces the mobilisation of $[Ca^{2+}]_i$, likely resulting in the activation of glutamate and nitric oxide signalling pathways, evoking in turn excitatory and inhibitory neuronal responses, respectively.

ETs increase $[Ca^{2+}]_i$ levels in SON astrocytes

Our results show that ET-1 induces robust and transient increases in $[Ca^{2+}]_i$ levels in SON astrocytes via mobilisation of thaspigargin-sensitive intracellular Ca^{2+} stores. Given that intracellular Ca^{2+} is a critical signalling modality in brain astrocytes (60), our studies suggest that ET-1 is an effective peptidergic modulator of astroglial function in the magnocellular neurosecretory system. This is in general agreement with previous studies in astrocyte cultures or astrocytes *in situ*, showing broad effects of ETs on astrocytic function, including activation (48,61), proliferation (35) changes in $[Ca^{2+}]_i$ levels (37,38) and changes in gap junction permeability (36,38), amongst others (19). On the other hand, our results differ from those recently reported by Zampronio *et al.* (19), who reported a lack of astrocyte Ca^{2+} responses to bath-applied ET-1 in the SON. The reasons underlying the discrepancy between these two studies are unclear, considering that similar ET-1 concentrations, rat strain and ages, and Ca^{2+}-sensitive dyes, were used in both studies. On the other hand, we speculate that methodological differences, including acquisition sampling rates or loading protocols, may have prevented the detection of ET-induced Ca^{2+} transients by Zampronio *et al.* (19).

Similar to previous reports in astrocytes in other brain regions (33,48,62–64), our studies support a contribution of ET_B receptors to the actions of ETs in the magnocellular neurosecretory system. We found that the selective ET_B receptor blocker BQ-788 diminished the number of ET-1 responsive astrocytes by approximately 75%. Moreover, similar responses to those evoked by ET-1 were observed when the selective ET_B receptor agonist S6c was used. Importantly, a combination of a selective ET_B and ET_A receptor blockers completely abolished the ET-1-mediated effects, supporting a contribution of ET_A receptors as well. Given the presence of different types of astrocytes in the magnocellular system (65), it would be important to determine whether anatomically and/or functionally distinct sets of astrocytes express different types of ETs receptors. Finally, the potential contribution of nonconventional ETs receptors (so-called 'atypical' receptors) (66,67) should also be considered, given recent studies showing these 'atypical' receptors to mediate the modulatory actions of ETs on hypothalamic catecholaminergic transmission (5,68,69).

An important caveat in the present study that needs to be taken into consideration is that the effect of ET-1 on astrocytes could be secondary to a potential vasoconstrictor effect. Although we cannot completely rule out this alternative, the fact that astrocytic Ca^{2+} changes persisted in the presence of papaverine, an approach extensively used to block ET-1-mediated vasoconstrictor effects (47), argues against this possibility. Moreover, it is well-established that ET-1-mediated vascular constriction in the cerebral circulation is predominantly mediated by ET_A receptors, whereas ET_B receptor activation may result in a vasodilatory effect (70–74). Thus, the fact that we observed similar changes in astrocytic Ca^{2+} between ET-1 and S6c (a selective ET_B receptor agonist), along with the fact that, in the slice preparation, blood vessels are almost maximally dilated under basal conditions, also argues against a vascular-mediated effect, particularly through ET_B receptor activation. Further studies, however, would be needed to prove this point more conclusively.

Changes in astrocytic Ca^{2+} can lead to activation of a variety of downstream signalling mechanisms, including the release of a variety of neuroactive substances, such as nitric oxide, ATP and glutamate. Given that all these signals can influence the activity of magnocellular neurosecretory neurones (75–77), we investigated whether ETs affected MNC firing activity, and assessed the potential contribution of the activation of ET_B receptors in astrocytes.

ET_B receptor activation influences SON neuronal firing activity

Our results show that activation of ET_B receptors with the selective agonist S6c (78), efficiently affected the activity of MNCs. The majority of MNCs (approximately 75%) responded with an increase in firing discharge, whereas an inhibitory response was observed in the remainder. Whether these opposing actions involved different cell types and/or signalling pathways is discussed below. Several lines of evidence from our work suggest that the effects of ETs on neuronal firing are mediated indirectly, likely via activation of ET_B receptors in astrocytes. First, neuronal responses to S6c were observed after a relatively long delay (approximately 6 min), suggesting the activation of an intermediary signalling mechanism. Second, neuronal responses to S6c were prevented by the gliotoxin selective compound L-αAA (49–51). Third, selective chelation of Ca^{2+} in the recorded neurone (BAPTA in the patch pipette) failed to affect ET_B-mediated effects on firing discharge, a result that is in line with the lack of ET-1-mediated changes in neuronal intracellular Ca^{2+}. On the other hand, bath application of BAPTA-AM (a membrane permeant form that resulted in Ca^{2+} chelation both in neurones and astrocytes) or thapsigargin prevented ET_B-mediated neuronal responses. Taken together, our results suggest that the modulation of SON neuronal activity by ETs is mediated via an indirect, Ca^{2+}-dependent mechanism, likely involving activation of glial

ET_B receptors, and subsequent Ca^{2+}-dependent release of gliotransmitters (see below). Although our results argue against the contribution of a Ca^{2+}-dependent signalling mechanism originating from a neuronal source, this possibility cannot be completely ruled out. Indeed, Zampronio *et al.* (19) showed that the frequency of glutamate excitatory postsynaptic currents in VP neurones is influenced by ET-1 in an autocrine manner via the Ca^{2+}-dependent release of endocannabinoids.

Our immunohistochemical studies support the presence of ET_B immunoreactivity in SON neurones and astrocytes. However, given that we observed a diffuse rather than a more characteristic surface membrane puncta pattern associated with receptors, caution should be taken when interpreting these results. It is worth mentioning, however, that a similar diffuse ET_B (and ET_A) receptor immunostaining pattern was previously reported in cerebellum and optic nerve astrocytes (62,79,80), as well as in neurones and astrocytes in dorsal root ganglia (81). In our case, most ET_B immunoreactivity in SON neurones displayed a perinuclear and/or nuclear distribution, a finding in line with previous studies showing nuclear ET_B receptors in vascular smooth muscle cells, endothelial cells and cardiomyocytes (82). Our studies may then suggest that ET_B receptors in MNCs may be coupled to signalling mechanisms unrelated to the control of membrane excitability, such as the long-term regulation of gene expression and apoptosis, amongst others. It is worth noting, however, that ET-mediated increases in $[Ca^{2+}]_i$ were previously described in hippocampal and striatal neurones vulnerable to ischaemic insults (83,84).

Glutamate and nitric oxide contribute to excitatory and inhibitory actions of ETs on MNCs

Glutamate and nitric oxide are two of the major excitatory and inhibitory neurotransmitters, respectively, influencing the activity of MNCs and hormone release (77,85–87). Given that these two neuromodulators are produced and actively released in a Ca^{2+}-dependent manner by astrocytes (57–59), we investigated their participation in ET-mediated excitatory and inhibitory effects on the activity of MNCs.

Our results showing an absence of inhibitory ET_B-mediated responses in the presence of the nonselective NOS blocker L-NAME support nitric oxide as a key mediator of ET_B-dependent inhibitory responses in MNCs. These results are in general agreement with a recent study showing that endogenous nitric oxide inhibited the release of VP evoked by ET_B receptor activation in hypothalamic-neurohypophyseal explants (6). Moreover, activation of ET_B receptors was recently shown to stimulate glial nitric oxide production via mobilisation of $[Ca^{2+}]_i$ (88–90). Thus, these results further support the notion that cross-talk between ETs and nitric oxide within astroglial cells plays an important physiological role (91).

Our results showing an almost complete blockade of ET_B-mediated excitatory responses in the presence of ionotrophic glutamate receptor blockers support glutamate as a likely transmitter mediating the ET_B-increased firing discharge in MNCs. Although we cannot determine the sources of glutamate contributing to this effect, it is reasonable to speculate, based on all our studies, that ET_B signalling in astrocytes could lead to a glutamate-mediated increase in the activity of MNCs via alternative, non-mutually exclusive mechanisms. For example, ET_B receptor activation has been shown to inhibit glial glutamate uptake via mobilisation of thapsigargin-sensitive Ca^{2+} stores (92,93). This would result in a slow build up of ambient glutamate levels, increasing in turn the magnitude of extrasynaptic NMDA receptor activation (94), a mechanism recently shown to be present in MNCs as well (95). In addition, astrocytes can release glutamate in a Ca^{2+}-dependent manner, which could in turn activate postsynaptic NMDA receptors (96,97), or facilitate the presynaptic release of glutamate via activation of group 1 mGLuRs (98,99). Finally, astrocytes could postsynaptically enhance glutamate receptor efficacy in MNCs via the release of ATP (26) or D-serine (28). Future studies aiming to determine the contribution of each of these mechanisms are warranted.

Taken together, our results suggest that activation of ET_B receptors in SON astrocytes results in the mobilisation of intracellular Ca^{2+} stores. This action could lead in turn to the activation of an nitric oxide-inhibitory and a glutamate-excitatory dependent signalling mechanism, respectively, which subsequently affects the firing activity of MNCs. Although these studies support the idea that the actions of ETs in the SON are likely dependent on precise, although complex neuroglial communication modalities, significant functional and mechanistic questions remain to be answered. It would be important to determine, for example, whether ET_B receptor activation within individual astrocytes and/or neurones can activate both nitric oxide- and glutamate-dependent pathways. In this scenario, factors affecting the endogenous balance between these two opposing signals would determine the overall outcome of ET_B responses within individual SON neurones. Alternatively, ET_B receptors could be differently coupled to nitric oxide and glutamate signalling pathways within discrete sets of astrocytes and neurones. Our results showing similar responses to the ET_B receptor agonist in eGFP-positive and negative neurones (putative vasopressin and oxytocin, respectively) would argue against this possibility. Other aspects that deserve to be further explored in the future include the cellular sources of endogenous ETs within the magnocellular system. In the brain, ETs are ubiquitously produced by endothelial cells, neurones (including MNCs) and astrocytes (3,34,100). Thus, whether ETs act in an autocrine or paracrine manner (or both) in the control of the activity of MNCs remains to be determined. One possibility dictating the source of ETs from these various cell types may stem from the origin/type of signal that stimulates its release. For example, changes in blood flow or increased shear stress may lead to increased ET release from endothelial cells (101). Similarly, swelling or mechano-transduction may cause its release from astrocytes (102). Although ET-1 has also shown to be present in vasopressin- and oxytocin-containing secretory granules in MNCs (100), whether ET-1 is intranuclearly released in an activity-dependent manner, as is the case for the co-release of VP and dynorphin (103), remains to be determined. Altogether, these observations would suggest that the physiological consequences of the action of ETs on neuronal activity in the SON may not only be dependent on

the types of receptor activated, but also upon the conditions by which ETs are released within the brain.

Acknowledgements

This work was funded by an American Heart Grant AHA 0640092N (J.E.S.) and the Agencia Nacional de Promoción Cientifica y Técnica, ANPCyT PICT 38333 y Universidad de Buenos Aires, UBACyT B083 (to M.S.V. and G.P.). We would like to thank Drs Y. Ueta (University of Occupational and Environmental Health, Kitakyushu Japan) and D. Murphy (University of Bristol, Bristol UK) for their kind donation of the AVP-eGFP rat breeders.

Received 8 February 2011,
revised 11 October 2011,
accepted 12 October 2011

References

1 Davenport AP. International Union of Pharmacology. XXIX. Update on endothelin receptor nomenclature. *Pharmacol Rev* 2002; **54**: 219–226.
2 Watts SW. Endothelin receptors: what's new and what do we need to know? *Am J Physiol Regul Integr Comp Physiol* 2010; **298**: R254–R260.
3 Yanagisawa M, Kurihara H, Kimura S, Tomobe Y, Kobayashi M, Mitsui Y, Yazaki Y, Goto K, Masaki T. A novel potent vasoconstrictor peptide produced by vascular endothelial cells. *Nature* 1988; **332**: 411–415.
4 Kuwaki T, Cao WH, Kumada M. Endothelin in the brain and its effect on central control of the circulation and other functions. *Jpn J Physiol* 1994; **44**: 1–18.
5 Perfume G, Nabhen SL, Barrera KR, Otero MG, Bianciotti LG, Vatta MS. Long-term modulation of tyrosine hydroxylase activity and expression by endothelin-1 and -3 in the rat anterior and posterior hypothalamus. *Am J Physiol Regul Integr Comp Physiol* 2008; **294**: R905–R914.
6 Rossi NF, Beierwaltes WH. Nitric oxide modulation of ET(B) receptor-induced vasopressin release by rat and mouse hypothalamo-neurohypophyseal explants. *Am J Physiol Regul Integr Comp Physiol* 2006; **290**: R1208–R1215.
7 Yamamoto T, Kimura T, Ota K, Shoji M, Inoue M, Sato K, Ohta M, Yoshinaga K. Central effects of endothelin-1 on vasopressin and atrial natriuretic peptide release and cardiovascular and renal function in conscious rats. *J Cardiovasc Pharmacol* 1991; **17**(Suppl 7): S316–S318.
8 Ritz MF, Stuenkel EL, Dayanithi G, Jones R, Nordmann JJ. Endothelin regulation of neuropeptide release from nerve endings of the posterior pituitary. *Proc Natl Acad Sci USA* 1992; **89**: 8371–8375.
9 Rossi NF. Regulation of vasopressin secretion by ETA and ETB receptors in compartmentalized rat hypothalamo-neurohypophysial explants. *Am J Physiol Endocrinol Metab* 2004; **286**: E535–E541.
10 Rossi NF, O'Leary DS, Chen H. Mechanisms of centrally administered ET-1-induced increases in systemic arterial pressure and AVP secretion. *Am J Physiol* 1997; **272**: E126–E132.
11 Rossi NF, O'Leary DS, Scislo TJ, Caspers ML, Chen H. Central endothelin 1 regulation of arterial pressure and arginine vasopressin secretion via the AV3V region. *Kidney Int Suppl* 1997; **61**: S22–S26.
12 Samson WK, Skala KD, Alexander BD, Huang FL. Hypothalamic endothelin: presence and effects related to fluid and electrolyte homeostasis. *J Cardiovasc Pharmacol* 1991; **17**(Suppl 7): S346–S349.
13 MacCumber MW, Ross CA, Glaser BM, Snyder SH. Endothelin: visualization of mRNAs by in situ hybridization provides evidence for local action. *Proc Natl Acad Sci USA* 1989; **86**: 7285–7289.
14 Takahashi K, Ghatei MA, Jones PM, Murphy JK, Lam HC, O'Halloran DJ, Bloom SR. Endothelin in human brain and pituitary gland: presence of immunoreactive endothelin, endothelin messenger ribonucleic acid, and endothelin receptors. *J Clin Endocrinol Metab* 1991; **72**: 693–699.
15 Yoshizawa T, Shinmi O, Giaid A, Yanagisawa M, Gibson SJ, Kimura S, Uchiyama Y, Polak JM, Masaki T, Kanazawa I. Endothelin: a novel peptide in the posterior pituitary system. *Science* 1990; **247**: 462–464.
16 Wall KM, Ferguson AV. Endothelin acts at the subfornical organ to influence the activity of putative vasopressin and oxytocin-secreting neurons. *Brain Res* 1992; **586**: 111–116.
17 Wall KM, Nasr M, Ferguson AV. Actions of endothelin at the subfornical organ. *Brain Res* 1992; **570**: 180–187.
18 Rossi NF, Chen H. PVN lesions prevent the endothelin 1-induced increase in arterial pressure and vasopressin. *Am J Physiol Endocrinol Metab* 2001; **280**: E349–E356.
19 Zampronio AR, Kuzmiski JB, Florence CM, Mulligan SJ, Pittman QJ. Opposing actions of endothelin-1 on glutamatergic transmission onto vasopressin and oxytocin neurons in the supraoptic nucleus. *J Neurosci* 2010; **30**: 16855–16863.
20 Yamamoto S, Inenaga K, Kannan H, Eto S, Yamashita H. The actions of endothelin on single cells in the anteroventral third ventricular region and supraoptic nucleus in rat hypothalamic slices. *J Neuroendocrinol* 1993; **5**: 427–434.
21 Poulain DA, Wakerley JB. Electrophysiology of hypothalamic magnocellular neurones secreting oxytocin and vasopressin. *Neuroscience* 1982; **7**: 773–808.
22 Bourque CW, Oliet SH, Kirkpatrick K, Richard D, Fisher TE. Extrinsic and intrinsic modulatory mechanisms involved in regulating the electrical activity of supraoptic neurons. *Ann NY Acad Sci* 1993; **689**: 512–519.
23 Theodosis DT, Piet R, Poulain DA, Oliet SH. Neuronal, glial and synaptic remodeling in the adult hypothalamus: functional consequences and role of cell surface and extracellular matrix adhesion molecules. *Neurochem Int* 2004; **45**: 491–501.
24 Hatton GI. Dynamic neuronal-glial interactions: an overview 20 years later. *Peptides* 2004; **25**: 403–411.
25 El Majdoubi M, Poulain DA, Theodosis DT. Lactation-induced plasticity in the supraoptic nucleus augments axodendritic and axosomatic GABAergic and glutamatergic synapses: an ultrastructural analysis using the disector method. *Neuroscience* 1997; **80**: 1137–1147.
26 Gordon GR, Baimoukhametova DV, Hewitt SA, Rajapaksha WR, Fisher TE, Bains JS. Norepinephrine triggers release of glial ATP to increase postsynaptic efficacy. *Nat Neurosci* 2005; **8**: 1078–1086.
27 Oliet SH, Piet R, Poulain DA. Control of glutamate clearance and synaptic efficacy by glial coverage of neurons. *Science* 2001; **292**: 923–926.
28 Panatier A, Theodosis DT, Mothet JP, Touquet B, Pollegioni L, Poulain DA, Oliet SH. Glia-derived D-serine controls NMDA receptor activity and synaptic memory. *Cell* 2006; **125**: 775–784.
29 Stern JE, Zhang W. Cellular sources, targets and actions of constitutive nitric oxide in the magnocellular neurosecretory system of the rat. *J Physiol* 2005; **562**: 725–744.
30 Sasaki Y, Takimoto M, Oda K, Fruh T, Takai M, Okada T, Hori S. Endothelin evokes efflux of glutamate in cultures of rat astrocytes. *J Neurochem* 1997; **68**: 2194–2200.
31 Lazarini F, Strosberg AD, Couraud PO, Cazaubon SM. Coupling of ETB endothelin receptor to mitogen-activated protein kinase stimulation and DNA synthesis in primary cultures of rat astrocytes. *J Neurochem* 1996; **66**: 459–465.
32 Jiang MH, Hoog A, Ma KC, Nie XJ, Olsson Y, Zhang WW. Endothelin-1-like immunoreactivity is expressed in human reactive astrocytes. *Neuroreport* 1993; **4**: 935–937.
33 Hori S, Komatsu Y, Shigemoto R, Mizuno N, Nakanishi S. Distinct tissue distribution and cellular localization of two messenger ribonucleic acids encoding different subtypes of rat endothelin receptors. *Endocrinology* 1992; **130**: 1885–1895.

34 Ehrenreich H, Kehrl JH, Anderson RW, Rieckmann P, Vitkovic L, Coligan JE, Fauci AS. A vasoactive peptide, endothelin-3, is produced by and specifically binds to primary astrocytes. *Brain Res* 1991; **538**: 54–58.

35 MacCumber MW, Ross CA, Snyder SH. Endothelin in brain: receptors, mitogenesis, and biosynthesis in glial cells. *Proc Natl Acad Sci USA* 1990; **87**: 2359–2363.

36 Giaume C, Cordier J, Glowinski J. Endothelins inhibit junctional permeability in cultured mouse astrocytes. *Eur J Neurosci* 1992; **4**: 877–881.

37 Fiacco TA, Agulhon C, Taves SR, Petravicz J, Casper KB, Dong X, Chen J, McCarthy KD. Selective stimulation of astrocyte calcium in situ does not affect neuronal excitatory synaptic activity. *Neuron* 2007; **54**: 611–626.

38 Blomstrand F, Giaume C, Hansson E, Ronnback L. Distinct pharmacological properties of ET-1 and ET-3 on astroglial gap junctions and Ca(2+) signaling. *Am J Physiol* 1999; **277**: C616–C627.

39 Ueta Y, Fujihara H, Serino R, Dayanithi G, Ozawa H, Matsuda K, Kawata M, Yamada J, Ueno S, Fukuda A, Murphy D. Transgenic expression of enhanced green fluorescent protein enables direct visualization for physiological studies of vasopressin neurons and isolated nerve terminals of the rat. *Endocrinology* 2005; **146**: 406–413.

40 Stern JE. Electrophysiological and morphological properties of pre-autonomic neurones in the rat hypothalamic paraventricular nucleus. *J Physiol* 2001; **537**: 161–177.

41 Sonner PM, Filosa JA, Stern JE. Diminished A-type potassium current and altered firing properties in presympathetic PVN neurones in renovascular hypertensive rats. *J Physiol* 2008; **586**: 1605–1622.

42 Biancardi VC, Campos RR, Stern JE. Altered balance of gamma-aminobutyric acidergic and glutamatergic afferent inputs in rostral ventrolateral medulla-projecting neurons in the paraventricular nucleus of the hypothalamus of renovascular hypertensive rats. *J Comp Neurol* 2010; **518**: 567–585.

43 Sonner PM, Stern JE. Functional role of A-type potassium currents in rat presympathetic PVN neurones. *J Physiol* 2007; **582**: 1219–1238.

44 Blanco VM, Stern JE, Filosa JA. Tone-dependent vascular responses to astrocyte-derived signals. *Am J Physiol Heart Circ Physiol* 2008; **294**: H2855–H2863.

45 Lohr C, Deitmer JW. *Ca^{2+} Imaging of Glia*. New York: Humana Press, 2010.

46 Ishikawa K, Ihara M, Noguchi K, Mase T, Mino N, Saeki T, Fukuroda T, Fukami T, Ozaki S, Nagase T, Nishikive M, Yano N. Biochemical and pharmacological profile of a potent and selective endothelin B-receptor antagonist, BQ-788. *Proc Natl Acad Sci USA* 1994; **91**: 4892–4896.

47 Lillestll IK, Helle KB, Aardal S. Relaxing effects of cyclic GMP and cyclic AMP-enhancing agents on the long-lasting contraction to endothelin-1 in the porcine coronary artery. *Scand J Clin Lab Invest* 1998; **58**: 625–634.

48 Ishikawa N, Takemura M, Koyama Y, Shigenaga Y, Okada T, Baba A. Endothelins promote the activation of astrocytes in rat neostriatum through ET(B) receptors. *Eur J Neurosci* 1997; **9**: 895–901.

49 Bridges RJ, Hatalski CG, Shim SN, Cummings BJ, Vijayan V, Kundi A, Cotman CW. Gliotoxic actions of excitatory amino acids. *Neuropharmacology* 1992; **31**: 899–907.

50 Olney JW, Ho OL, Rhee V. Cytotoxic effects of acidic and sulphur containing amino acids on the infant mouse central nervous system. *Exp Brain Res* 1971; **14**: 61–76.

51 Xu HL, Ye S, Baughman VL, Feinstein DL, Pelligrino DA. The role of the glia limitans in ADP-induced pial arteriolar relaxation in intact and ovariectomized female rats. *Am J Physiol Heart Circ Physiol* 2005; **288**: H382–H388.

52 Alvarez-Maubecin V, Garcia-Hernandez F, Williams JT, Van Bockstaele EJ. Functional coupling between neurons and glia. *J Neurosci* 2000; **20**: 4091–4098.

53 Baudoux S, Parker D. Glial-toxin-mediated disruption of spinal cord locomotor network function and its modulation by 5-HT. *Neuroscience* 2008; **153**: 1332–1343.

54 McBean GJ. Inhibition of the glutamate transporter and glial enzymes in rat striatum by the gliotoxin, alpha aminoadipate. *Br J Pharmacol* 1994; **113**: 536–540.

55 Xu HL, Mao L, Ye S, Paisansathan C, Vetri F, Pelligrino DA. Astrocytes are a key conduit for upstream signaling of vasodilation during cerebral cortical neuronal activation in vivo. *Am J Physiol Heart Circ Physiol* 2008; **294**: H622–H632.

56 Filosa JA, Blanco VM. Neurovascular coupling in the mammalian brain. *Exp Physiol* 2007; **92**: 641–646.

57 Ni Y, Malarkey EB, Parpura V. Vesicular release of glutamate mediates bidirectional signaling between astrocytes and neurons. *J Neurochem* 2007; **103**: 1273–1284.

58 Sporbert A, Mertsch K, Smolenski A, Haseloff RF, Schonfelder G, Paul M, Ruth P, Walter U, Blasig IE. Phosphorylation of vasodilator-stimulated phosphoprotein: a consequence of nitric oxide- and cGMP-mediated signal transduction in brain capillary endothelial cells and astrocytes. *Brain Res Mol Brain Res* 1999; **67**: 258–266.

59 Gabbott PL, Bacon SJ. Localisation of NADPH diaphorase activity and NOS immunoreactivity in astroglia in normal adult rat brain. *Brain Res* 1996; **714**: 135–144.

60 Agulhon C, Petravicz J, McMullen AB, Sweger EJ, Minton SK, Taves SR, Casper KB, Fiacco TA, McCarthy KD. What is the role of astrocyte calcium in neurophysiology? *Neuron* 2008; **59**: 932–946.

61 Barone FC, Willette RN, Yue TL, Feurestein G. Therapeutic effects of endothelin receptor antagonists in stroke. *Neurol Res* 1995; **17**: 259–264.

62 Furuya S, Hiroe T, Ogiso N, Ozaki T, Hori S. Localization of endothelin-A and -B receptors during the postnatal development of rat cerebellum. *Cell Tissue Res* 2001; **305**: 307–324.

63 Hama H, Sakurai T, Kasuya Y, Fujiki M, Masaki T, Goto K. Action of endothelin-1 on rat astrocytes through the ETB receptor. *Biochem Biophys Res Commun* 1992; **186**: 355–362.

64 Hosli E, Hosli L. Autoradiographic evidence for endothelin receptors on astrocytes in cultures of rat cerebellum, brainstem and spinal cord. *Neurosci Lett* 1991; **129**: 55–58.

65 Bonfanti L, Poulain DA, Theodosis DT. Radial glia-like cells in the supraoptic nucleus of the adult rat. *J Neuroendocrinol* 1993; **5**: 1–5.

66 Jensen N, Hasselblatt M, Siren AL, Schilling L, Schmidt M, Ehrenreich H. ET(A) and ET(B) specific ligands synergistically antagonize endothelin-1 binding to an atypical endothelin receptor in primary rat astrocytes. *J Neurochem* 1998; **70**: 473–482.

67 Ehrenreich H. The astrocytic endothelin system: toward solving a mystery focus on 'distinct pharmacological properties of ET-1 and ET-3 on astroglial gap junctions and Ca(2+) signaling'. *Am J Physiol* 1999; **277**: C614–C615.

68 Hope SI, Nabhen SL, Soria C, Bianciotti LG, Vatta MS. Endothelin-1 and -3 modulate the neuronal norepinephrine transporter through multiple signalling pathways in the rat posterior hypothalamus. *Neurochem Int* 2010; **57**: 306–313.

69 Perfume G, Morgazo C, Nabhen S, Batistone A, Hope SI, Bianciotti LG, Vatta MS. Short-term regulation of tyrosine hydroxylase activity and expression by endothelin-1 and endothelin-3 in the rat posterior hypothalamus. *Regul Pept* 2007; **142**: 69–77.

70 Hansen-Schwartz J, Edvinsson L. Increased sensitivity to ET-1 in rat cerebral arteries following organ culture. *Neuroreport* 2000; **11**: 649–652.

71 Kobari M, Fukuuchi Y, Tomita M, Tanahashi N, Konno S, Takeda H. Constriction/dilatation of the cerebral microvessels by intravascular endothelin-1 in cats. *J Cereb Blood Flow Metab* 1994; **14**: 64–69.

72 Robinson MJ, McCulloch J. Contractile responses to endothelin in feline cortical vessels in situ. *J Cereb Blood Flow Metab* 1990; **10**: 285–289.

73 Schilling L, Feger GI, Ehrenreich H, Wahl M. Endothelin-3-induced relaxation of isolated rat basilar artery is mediated by an endothelial ETB-type endothelin receptor. *J Cereb Blood Flow Metab* 1995; **15**: 699–705.

74 Touzani O, Galbraith S, Siegl P, McCulloch J. Endothelin-B receptors in cerebral resistance arterioles and their functional significance after focal cerebral ischemia in cats. *J Cereb Blood Flow Metab* 1997; **17**: 1157–1165.

75 Bull PM, Brown CH, Russell JA, Ludwig M. Activity-dependent feedback modulation of spike patterning of supraoptic nucleus neurons by endogenous adenosine. *Am J Physiol Regul Integr Comp Physiol* 2006; **291**: R83–R90.

76 Nissen R, Hu B, Renaud LP. Regulation of spontaneous phasic firing of rat supraoptic vasopressin neurones in vivo by glutamate receptors. *J Physiol* 1995; **484**: 415–424.

77 Stern JE, Ludwig M. NO inhibits supraoptic oxytocin and vasopressin neurons via activation of GABAergic synaptic inputs. *Am J Physiol Regul Integr Comp Physiol* 2001; **280**: R1815–R1822.

78 Williams DL Jr, Jones KL, Pettibone DJ, Lis EV, Clineschmidt BV. Sarafotoxin S6c: an agonist which distinguishes between endothelin receptor subtypes. *Biochem Biophys Res Commun* 1991; **175**: 556–561.

79 Rogers SD, Peters CM, Pomonis JD, Hagiwara H, Ghilardi JR, Mantyh PW. Endothelin B receptors are expressed by astrocytes and regulate astrocyte hypertrophy in the normal and injured CNS. *Glia* 2003; **41**: 180–190.

80 Schinelli S, Zanassi P, Paolillo M, Wang H, Feliciello A, Gallo V. Stimulation of endothelin B receptors in astrocytes induces cAMP response element-binding protein phosphorylation and c-fos expression via multiple mitogen-activated protein kinase signaling pathways. *J Neurosci* 2001; **21**: 8842–8853.

81 Plant TD, Zollner C, Kepura F, Mousa SS, Eichhorst J, Schaefer M, Furkert J, Stein C, Oksche A. Endothelin potentiates TRPV1 via ETA receptor-mediated activation of protein kinase C. *Mol Pain* 2007; **3**: 35.

82 Bkaily G, Avedanian L, Al-Khoury J, Provost C, Nader M, D'Orleans-Juste P, Jacques D. Nuclear membranes receptors for ET-1 in cardiovascular function. *Am J Physiol Regul Integr Comp Physiol* 2011; **300**: R251–R263.

83 Kataoka Y, Koizumi S, Niwa M, Shibaguchi H, Shigematsu K, Kudo Y, Taniyama K. Endothelin-3 stimulates inositol 1,4,5-trisphosphate production and Ca^{2+} influx to produce biphasic dopamine release from rat striatal slices. *Cell Mol Neurobiol* 1994; **14**: 271–280.

84 Koizumi S, Kataoka Y, Niwa M, Yamashita K, Taniyama K, Kudo Y. Endothelin increased $[Ca^{2+}]$i in cultured neurones and slices of rat hippocampus. *Neuroreport* 1994; **5**: 1077–1080.

85 Brown CH. Rhythmogenesis in vasopressin cells. *J Neuroendocrinol* 2004; **16**: 727–739.

86 Israel JM, Poulain DA, Oliet SH. Glutamatergic inputs contribute to phasic activity in vasopressin neurons. *J Neurosci* 2010; **30**: 1221–1232.

87 Kadekaro M, Summy-Long JY. Centrally produced nitric oxide and the regulation of body fluid and blood pressure homeostases. *Clin Exp Pharmacol Physiol* 2000; **27**: 450–459.

88 Morga E, Faber C, Heuschling P. Stimulation of endothelin B receptor modulates the inflammatory activation of rat astrocytes. *J Neurochem* 2000; **74**: 603–612.

89 Saadoun S, Garcia A. Endothelin stimulates nitric oxide-dependent cyclic GMP formation in rat cerebellar astroglia. *Neuroreport* 1999; **10**: 33–36.

90 Yamashita K, Kataoka Y, Sakurai-Yamashita Y, Shigematsu K, Himeno A, Niwa M, Taniyama K. Involvement of glial endothelin/nitric oxide in delayed neuronal death of rat hippocampus after transient forebrain ischemia. *Cell Mol Neurobiol* 2000; **20**: 541–551.

91 Hocher B, Schwarz A, Slowinski T, Bachmann S, Pfeilschifter J, Neumayer HH, Bauer C. In-vivo interaction of nitric oxide and endothelin. *J Hypertens* 2004; **22**: 111–119.

92 Leonova J, Thorlin T, Aberg ND, Eriksson PS, Ronnback L, Hansson E. Endothelin-1 decreases glutamate uptake in primary cultured rat astrocytes. *Am J Physiol Cell Physiol* 2001; **281**: C1495–C1503.

93 Matsuura S, Ikegaya Y, Yamada MK, Nishiyama N, Matsuki N. Endothelin downregulates the glutamate transporter GLAST in cAMP-differentiated astrocytes in vitro. *Glia* 2002; **37**: 178–182.

94 Le Meur K, Galante M, Angulo MC, Audinat E. Tonic activation of NMDA receptors by ambient glutamate of non-synaptic origin in the rat hippocampus. *J Physiol* 2007; **580**: 373–383.

95 Fleming TM, Scott V, Naskar K, Joe N, Brown CH, Stern JE. State-dependent changes in astrocyte regulation of extrasynaptic NMDA receptor signalling in neurosecretory neurons. *J Physiol* 2011; **589**: 3929–3941.

96 Araque A, Parpura V, Sanzgiri RP, Haydon PG. Glutamate-dependent astrocyte modulation of synaptic transmission between cultured hippocampal neurons. *Eur J Neurosci* 1998; **10**: 2129–2142.

97 Parpura V, Basarsky TA, Liu F, Jeftinija K, Jeftinija S, Haydon PG. Glutamate-mediated astrocyte-neuron signalling. *Nature* 1994; **369**: 744–747.

98 Fiacco TA, McCarthy KD. Intracellular astrocyte calcium waves in situ increase the frequency of spontaneous AMPA receptor currents in CA1 pyramidal neurons. *J Neurosci* 2004; **24**: 722–732.

99 Araque A, Perea G. Glial modulation of synaptic transmission in culture. *Glia* 2004; **47**: 241–248.

100 Nakamura S, Naruse M, Naruse K, Shioda S, Nakai Y, Uemura H. Colocalization of immunoreactive endothelin-1 and neurohypophysial hormones in the axons of the neural lobe of the rat pituitary. *Endocrinology* 1993; **132**: 530–533.

101 Kuchan MJ, Frangos JA. Shear stress regulates endothelin-1 release via protein kinase C and cGMP in cultured endothelial cells. *Am J Physiol* 1993; **264**: H150–H156.

102 Ostrow LW, Sachs F. Mechanosensation and endothelin in astrocytes–hypothetical roles in CNS pathophysiology. *Brain Res Brain Res Rev* 2005; **48**: 488–508.

103 Brown CH, Bourque CW. Autocrine feedback inhibition of plateau potentials terminates phasic bursts in magnocellular neurosecretory cells of the rat supraoptic nucleus. *J Physiol* 2004; **557**: 949–960.